IEEE Access
Multidisciplinary | Rapid Review | Open Access Journal

Received August 25, 2018, accepted September 26, 2018, date of publication October 4, 2018, date of current version October 29, 2018.

Digital Object Identifier 10.1109/ACCESS.2018.2873721

Design and Evaluation of Optimal Orthogonal Wavelet With the Least Length of Wavelet Filters Using Spectral Matching

MAHMOUD MANSOURI JAM AND HAMED SADJEDI
[1]Department of Electrical Engineering, Shahed University, Tehran 1865133191, Iran
Corresponding author: Hamed Sadjedi (sadjedi@shahed.ac.ir)

ABSTRACT This paper presents a method to find a matched wavelet with the least length of wavelet filters using spectral matching. The existing problem in algorithm of designing in spectral fashion is described, and the corresponding solution is provided. The problem encountered in the common algorithm is the heavy computations in spectral phase matching that often produces errors in machine running, and consequently, the phase matching algorithm becomes incomplete. In this paper, the computational costs and errors arising from such phase matching are improved. Then, a method is proposed, thereby enabling the construction of orthogonal wavelet transform filters with minimum length. The proposed approach is examined with a signal from the real world. The compression of neural signals in implantable microsystems is provided, and its performance is compared with the superior wavelets. It yields higher compression rate than other well-reported wavelets, such as *sym*4, *db*4, and *sym*7, as well as the designed wavelet is able to perform more efficient than general wavelets in noisy conditions. These appropriate results are obtained because of designing matched wavelet with the least length of filters.

INDEX TERMS Compression, matched wavelet, multi-resolution analysis (MRA), orthogonal.

I. INTRODUCTION

The designing an appropriate wavelet basis for a specified signal has been a long-standing issue in various studies. Some well-documented wavelets such as Daubechies fashion are methods for designing the general wavelets, not for matched wavelet to specified signal. In many applications such as signal activity detection [1], signal coding [2], signal compression [3], using a matched wavelet for a specified signal is efficient and presents favorable results.

In [4], Mallat and Zhang presented a technique called matching pursuit, which uses a dictionary of pre-defined scaling functions for the matching process. The process currently adopted by many researchers involves the selection of a library of existing wavelet bases and the determination and optimization of a cost function [5]. Some of them propose the algorithms proper only for continuous wavelet transform (CWT), such as generalized Mexican-hat function [6]. In discrete wavelet transform (DWT), most methods for designing matched wavelets use techniques that emphasize on computation of wavelet filter to generate scale functions and provide no criteria for the direct matching of wavelet functions. For instances, the trigonometric parameterization of the of wavelet filter was used in [7] and [8]. In some studies, the minimization of the least mean error of decomposition with respect to wavelet filter was used [9], [10]. In [11], the heuristic optimization algorithms were proposed for searching the best values of parameters of the wavelet.

Another approach is directly matching orthonormal wavelets to a desired signal without the application of pre-conditions on the signal's waveform. In [12], a framework was developed for designing of matched wavelets in the time-domain. Another framework is based on designing of matched wavelets in the frequency domain. In the latter framework, an optimal algorithm was presented in [13] (from now on, it is recalled as primary algorithm). Using this primary algorithm, an orthonormal matched wavelet in multi-resolution analysis (MRA) can be matched directly to its corresponding specified signal. This algorithm directly matches the band-limited frequency spectrum of a wavelet to the spectrum of a specified signal, by minimizing the mean square error. It has been adopted in a number of applications, such as in Electrocardiography (ECG) [14], ball-bearing fault detection [15], and medical image processing [16].

Despite the capabilities of this algorithm, it has been employed in only a few studies because of some hidden problems.

This paper, firstly, presents the detection and addressing of the problem encountered in the primary algorithm, and proposes the corresponding solution. In general, the full spectrum of a signal consists of its amplitude and its phase. Correct matching requires the consideration of both parts. The most of previous works have not achieved to full matched wavelet in both of amplitude and phase sections simultaneously [15]–[17]. The main problem is that the primary algorithm suffers from heavy computational spectral phase matching [18] that often produces errors in machine running, thereby the phase matching algorithm is not accomplished. Secondly, the primary algorithm generates very wide length of wavelet filters; as indicated in [15], this feature may lead one to believe that the wavelet has no limited support. The wide length of wavelet filters prevents the usage in many situations such as in applications with hardware constraints such as in some implantable microsystems. In this study, a modification is provided for the primary algorithm and thereby the problem of phase matching is solved, as well, a designing method is proposed to generate the least length of wavelet filters. The efficiency of the proposed solutions is verified on an example of real world applications, i.e. neural signal compression that it is our current underlying study.

Section II provides an overview of the primary algorithm. Section III describes the details of problems and proposed solutions. To verify the solutions, section IV tests three examples. Section V discussed about performance evaluation of the proposed approach. Section VI concludes the paper.

II. PRELIMINARIES

Because this paper deals with the mid-points of the primary algorithm and the proposed techniques depend on some formulas in middle of the primary algorithm [13], [19], a brief review of the primary algorithm is necessary. The review of some formulas may be tedious for some readers, however, the key problems of the primary algorithm are situated delicately in depth of the algorithm. Therefore, it is inevitable to brief review of it, in the main text, to clarify subtly which part is the origin of the problem. For a MRA there is a pair of relations as [20], [21]:

$$\phi(x) = 2\sum_{k} h_k \phi(2k - x) \tag{1}$$

$$\psi(x) = 2\sum_{k} g_k \phi(2k - x) \tag{2}$$

where $\psi(x)$ is wavelet and $\varphi(x)$ is scaling function. The h_k and g_k are the coefficients of Quadrature Mirror Filters (QMF) for the MRA. In frequency domain, there are:

$$\Phi(\omega) = H\left(\frac{\omega}{2}\right)\Phi\left(\frac{\omega}{2}\right) \tag{3}$$

$$\Psi(\omega) = G\left(\frac{\omega}{2}\right)\Phi\left(\frac{\omega}{2}\right) \tag{4}$$

The final outputs of Orthonormal MRA (OMRA) are the coefficients of the h and g filters. Deriving these outputs necessitates a scale function. When the goal is to directly obtain matched wavelets from a given signal, a $\Psi(\omega)$ is derived, while a closed form relationship to obtain a $\Phi(\omega)$ from a $\Psi(\omega)$ does not exist. The primary algorithm presented algorithms, in which the spectrally amplitude and phase of $\Phi(\omega)$ are obtained. Firstly, for a given signal or $f(x)$, amplitude of matched wavelet function, $|\Psi(\omega)|$, is obtained and thereby $|\Phi(\omega)|$ is obtained as follows:

$$|\Phi(2\omega)|^2 = \sum_{k=1}^{\infty} \left|\Psi\left(2^k\omega\right)\right|^2, \quad (for\ \omega \neq 0) \tag{5}$$

Secondly, the phases of $\Psi(\omega)$ and $\Phi(\omega)$ are obtained through an algorithm. With combination of them, the full spectrum of $\Psi(\omega)$ and $\Phi(\omega)$, and consequently h and g filters are obtained. To guarantee that a wavelet function satisfies OMRA conditions, two issues must be considered: the orthonormality of the function and the satisfaction of MRA conditions. If the following relationship is satisfied, then the orthonormality of the $\Psi(\omega)$ is guaranteed:

$$\sum_{m=-\infty}^{\infty} |\Phi(\omega + 2m\pi)|^2 = 1$$

$$\Rightarrow \sum_{m=-\infty}^{\infty}\sum_{k=1}^{\infty} \left|\Psi\left(2^k(\omega + 2m\pi)\right)\right|^2 = 1 \tag{6}$$

To ensure that MRA conditions are imposed on the matched wavelet, with the proofs of two theorems in [19], $\Psi(\omega)$ and $\Phi(\omega)$ must be characterized as follows:

$$\begin{aligned} &\Phi(\omega) \neq 0; \quad for\ |\omega| < 4\pi/3 \\ &\Psi(\omega) \neq 0; \quad for\ 2\pi/3 < |\omega| < 8\pi/3 \end{aligned} \tag{7}$$

The primary algorithm in two sections is reviewed. The first section presents the design of matched amplitude. We emphasize on second section, the design of matched phase, because it is the origin of the problem.

A. ALGORITHM FOR MATCHED AMPLITUDE

Let the spectral sampling resolution of $\Phi(\omega)$ and $\Psi(\omega)$ are $\Delta\omega_\Phi = 2\pi/2^{l+1}$ and $\Delta\omega_\Psi = 2\pi/2^M$, respectively, then $\Phi(\omega)$ and $\Psi(\omega)$ are discretized as $\Phi(n\Delta\omega_\Phi)$ and $\Psi(n\Delta\omega_\Psi)$. Now, the (5) and (6) are discretized:

$$\left|\Phi\left(\frac{\pi n}{2^l}\right)\right|^2 = \sum_{p=0}^{l}\left|\Psi\left(\frac{2\pi n}{p}\right)\right|^2 \tag{8}$$

$$\sum_{m=-\infty}^{\infty}\sum_{p=0}^{l}\left|\Psi\left(\frac{2^M}{2^p}\left(n + 2^{l+1}m\right)\right)\right|^2 = 1 \tag{9}$$

Applying the guarantee constraints for MRA, i.e., the range of frequency bands authorized for $\Psi(\omega)$ in (7), indicates that (9) has value only in the following range:

$$\frac{2^{M-1}}{3} < \frac{2^M}{2^p}\left(n + 2^{l+1}m\right) < \frac{2^{M+2}}{3} \tag{10}$$

We assume that the designed wavelet function is real, then its spectrum is an even function. Thus, computation only for the frequency of positive indices is sufficient. If $\Psi(\omega)$ is matched in the k point of spectra, and $Y(k)$ shows the sampled power spectrum of $\Psi(\omega)$, finding $Y(k) = |\Psi(k\Delta\omega)|^2$ requires L linear equations, such that

$$\sum_{i=1}^{k} \alpha_{ij} Y(k) = 1 \tag{11}$$

where k$\varepsilon\{2^M/3, \ldots, 2^{M+2}/3\}$. The (11) can be written in vector form as $\mathbf{A}Y=1$, in which matrix $\mathbf{A}$ is set as $\mathbf{A}=\{\alpha_{ij}\epsilon\{0,1,2\}\}$, and 1 is a unity vector of length L. If $W(k)$ is the sampled power spectrum of $F(\omega)$, and we define $W(k) = |F(k)|^2$ to derive an appropriate $Y(k)$, E or the normalized mean square error between $Y(k)$ and $W(k)$ is minimized. Therefore,

$$E = \frac{\sum_k (W(k) - Y(k))^2}{\sum_k W(k)^2} \tag{12}$$

With the Lagrangian multiplier and a weighting parameter a, error E can be minimized, after which

$$Y = \frac{1}{a}W + \mathbf{A}^T \left(\mathbf{A}\mathbf{A}^T\right)^{-1} \left(1 - \frac{1}{a}\mathbf{A}W\right) \tag{13}$$

Now, the power spectrum of matched wavelet can be computed from $|\Psi(k\Delta\omega)|^2 = Y(k)$, and from (8) amplitude of the scale function can be computed.

B. ALGORITHM FOR MATCHED PHASE

For the phase matching, a direct matching process is not possible. To solve this problem, group delay is considered. The phases of $\Phi(\omega)$ and $\Psi(\omega)$ are given by

$$\theta_\Phi(\omega) = \sum_{m=1}^{\infty} \theta_H\left(\frac{\omega}{2^m}\right) \tag{14}$$

$$\theta_\Psi(\omega) = -\frac{\omega}{2} - \theta_H\left(\frac{\omega}{2} + \pi\right) + \sum_{m=2}^{\infty} \theta_H\left(\frac{\omega}{2^m}\right) \tag{15}$$

where θ_Ψ, θ_Φ, and θ_H are the phases of the $\Psi(\omega)$, $\Phi(\omega)$, and filter H, respectively. If $\lambda(\omega)$ is the negative group delay of filter H, then the negative group delay of the $\Phi(\omega)$ and $\Psi(\omega)$, (i.e., Δ_Φ and Δ_Ψ, respectively), are obtained from $\lambda(\omega)$ as follows:

$$\Lambda_\Phi(\omega) = \sum_{m=1}^{\infty} 2^{-m} \lambda\left(\frac{\omega}{2^m}\right) \tag{16}$$

$$\Lambda_\Psi(\omega) = -\frac{1}{2} - \frac{1}{2}\lambda\left(\frac{\omega}{2} + \pi\right) + \sum_{m=2}^{\infty} 2^{-m} \lambda\left(\frac{\omega}{2^m}\right) \tag{17}$$

If Γ_Ψ is defined as $\Gamma_\Psi = \Delta_\Psi + 1/2$, then

$$\Gamma_\Psi(\omega) = -\frac{1}{2}\lambda\left(\frac{\omega}{2} + \pi\right) + \sum_{m=2}^{\infty} 2^{-m} \lambda\left(\frac{\omega}{2^m}\right) \tag{18}$$

Phase matching involves dealing with $\lambda(\omega)$, which is 2π-periodic, and the problem of deriving θ_Φ from θ_Ψ remains. To solve them, function $\lambda(\omega)$ is modeled with *R-order* polynomials. Because $\lambda(\omega)$ is an even function, a polynomial is only an even phrase:

$$\lambda_T(\omega) = \sum_{r=0}^{R/2} c_r \omega^{2r} \Pi\left(\frac{\omega}{2\pi}\right),$$
$$rect: \Pi(\omega) = \begin{cases} 1; & -\frac{1}{2} \le \omega < \frac{1}{2} \\ 0; & elsewhere \end{cases} \tag{19}$$

Thus, $\lambda(\omega)$ is obtained as follows:

$$\lambda(\omega) = \sum_{k=-\infty}^{\infty} \lambda_T(\omega - 2k\pi)$$
$$= \sum_{k=-\infty}^{\infty} \sum_{r=0}^{R/2} c_r (\omega - 2k\pi)^{2r} \Pi\left(\frac{\omega - 2k\pi}{2\pi}\right) \tag{20}$$

If the spectral sampling resolution of H is $\Delta\omega = 2\pi/T$, and N is the number of samples in $F(n\Delta\omega)$, then the number of periods in N-point is $P = N/T$, and $-N/2 \le n < N/2$. Therefore, discrete case $\lambda(n)$ is derived thus:

$$\lambda(n) = \sum_{r=0}^{R/2} c_r \sum_{k=-P/2}^{P/2-1} (n - kT)^{2r} \Pi\left(\frac{n - kT}{T}\right) \tag{21}$$

The matrix form of (21) is $\lambda = \mathbf{B}c$, where the elements of matrix $\mathbf{B}$ are given by:

$$b_{n,r} = \sum_{k=-P/2}^{P/2-1} (n - kT)^{2r} \Pi\left(\frac{n - kT}{T}\right) \tag{22}$$

Therefore, the matrix form of $\Gamma_\Psi(\omega)$ and $\mathbf{\Delta}_\Phi(\omega)$ are

$$\mathbf{\Gamma}_\Psi = \mathbf{D}_\Psi c, \quad where: \mathbf{D}_\Psi = -\frac{1}{2}\mathbf{B}_{\frac{n+T}{2}} + \sum_{m=2}^{\infty} 2^{-m}\mathbf{B}_{\frac{1}{2^m}} \tag{23}$$

$$\mathbf{\Lambda}_\Phi = \mathbf{D}_\Phi c, \quad where: \mathbf{D}_\Phi = \sum_{m=1}^{\infty} 2^{-m}\mathbf{B}_{\frac{1}{2^m}} \tag{24}$$

Because group delay needs to be matched only in the range wherein the amplitude spectrum of the wavelet function exists, such delay can be weighted using $\Omega(n) = Y(n)/\sum Y(n)$. Therefore, the cost function defined as:

$$\gamma = \sum_{n=-N/2}^{N/2-1} [\Omega(n)(\mathbf{\Gamma}_F(n) - \mathbf{\Gamma}_\Psi(n))]^2$$
$$= \sum_{n=-N/2}^{N/2-1} \left[\Omega(n)\left(\mathbf{\Gamma}_F(n) - \sum_{r=0}^{R/2} c_r d_{n,r}\right)\right]^2 \tag{25}$$

where $d_{n,r}$ are the elements of matrix $\mathbf{D}_\Psi$. Defining $\mathbf{\Gamma}_F^*$ instead of $\{\Omega(n)\mathbf{\Gamma}_F(n)\}$ and $\mathbf{D}_\Psi^*$ instead of $\{\Omega(n)d_{n,r}\}$ in matrix form yields

$$\gamma = (\mathbf{\Gamma}_F^* - \mathbf{D}_\Psi^* c)^T \left(\mathbf{\Gamma}_F^* - \mathbf{D}_\Psi^* c\right) \tag{26}$$

Using the derivative of γ with respect to c yields the optimum c coefficients obtained by linear least squares:

$$c = \left(\mathbf{D}_{\Psi}^{*T}\mathbf{D}_{\Psi}^{*}\right)^{-1}\mathbf{D}_{\Psi}^{*T}\mathbf{\Gamma}_{F}^{*} \tag{27}$$

Obtaining c enables the derivation of the group delay of the $\Psi(\omega)$, $\Phi(\omega)$, and H as follows:

$$\mathbf{\Lambda}_{\Psi} = \mathbf{D}_{\Psi}c - \frac{1}{2}, \quad \mathbf{\Lambda}_{\Phi} = \mathbf{D}_{\Phi}c, \quad \lambda = Bc \tag{28}$$

With the integration of the acquired group delays, θ_{Ψ} and θ_{Φ} are obtained. Through the matched amplitude and matched phase of the $\Psi(\omega)$,(i.e., $|Y(n)|^{1/2}$ and θ_{Ψ}, respectively), as well as through the matched amplitude and matched phase of the $\Phi(\omega)$, the full spectrum of the discretized $\Psi(\omega)$ and $\Phi(\omega)$ are computed. At the end, the H and G are obtained using (3) and (4) as final outputs [13], [19].

III. PROBLEMS IN IMPLEMENTATION OF THE PRIMARY ALGORITHM AND CORRESPONDING SOLUTIONS

Some works have used the primary algorithm to design matched wavelet. Few of them used CWT, which basically disregards OMRA; in CWT fashion, $\varphi(x)$, h, and g are not required and only finding of $\psi(x)$ is sufficient, therefore they are not constructed in the normal fashion [19], [22]. By contrast, the DWT requires the h and g filters, however, it necessitates the existence of a scaling function $\varphi(x)$.

At the first point, it is worth noting that in the primary algorithm has been stated that for obtaining the H and G filters use (3) and (4). However, during obtaining the H filter by using of (3), the problem of dividing to zero occurs. To escape from this problem, we propose to use the original definition of the time domain relationship employed in MRA [17], not (3) and (4). Therefore, the coefficients of filter h can be obtained by using:

$$h_k = \sqrt{2}\sum_{n=0}^{N-1}\phi\left[n\right]\phi\left[n-k\right]. \tag{29}$$

The primary algorithm does not face any problem in amplitude section but faces problem in phase section. In phase section, there are two possible ways: obtaining the correctly matched phase, setting phase to zero (i.e. not-obtaining the matched phase). According to the properties of Fourier Transform, if a signal is real and even in time domain, it is purely real signal in frequency domain (i.e., having zero-phase). However, as indicated in some works such as in [15]–[17], the existence of realness and even symmetry in wavelet function and its filters, enables the determination that they have zero phase, and therefore they have not obtained a matched phase. In the other words, the previous works have not achieved to full matched wavelet in both of amplitude and phase sections [15]–[17]. In most actual applications, such as those involving neural spikes, ECG signals, and seismic signals, no symmetric signals exist [14], [15]. Appropriate and correct matching therefore inevitably requires obtaining the correct phase of $\Phi(\omega)$.

A. PROBLEM OF D_{Ψ} MATRIX AND SOLUTION

The exact and full implementation of the primary algorithm and the review of studies in which this algorithm was used, persuades us toward an important problem. It pertains to the heavy computational of spectral phase matching that is required in dealing with **B** and **D** matrices. These matrices have very large values and are characterized by unsuitable conditions. During algorithm implementation, therefore, they often cause errors in machine running, thereby the phase matching is not realized correctly. Therefore, case-studies often have used the setting θ_{Φ} to zero instead of using of correctly matching of θ_{Φ}.

To illustrate the $\mathbf{D}_{\Psi}$ matrix problem, let us suppose an example. Matching process requires the construction of matrix **B**, such that $\mathbf{D}_{\Psi}$ and $\mathbf{D}_{\Phi}$ be built from **B**. Our tests and some studies (e.g. [15], [16], [19]) show that the degree of a polynomial for group delay modeling, R, must exceed 16 to derive appropriate results. If the sampling frequency resolution is $\Delta\omega = 2\pi/16$, then T is 16, and if the number of samples N in $F(n)$ is 512, then range of n is $-256 \leq n < 256$. With regard to the term $(n\text{-}kT)^{2r}$ in (22), a wide range of numbers (from very small to very great) is expected in the computation of matrix elements. With values $N = 512$, $R = 16$, and $T = 16$, the size of $\mathbf{D}_{\Psi}$ is 512×9. The size of $\mathbf{D}_{\Psi}$ matrix is very large that it is not possible to present $\mathbf{D}_{\Psi}$ in matrix form in this paper; however, with a figure it can be possible to display the range of numbers in a column of this matrix. For instance, the ranges of numbers in a part of two columns of $\mathbf{D}_{\Psi}$ are illustrated in Fig. 1, those are, the elements of $\mathbf{D}_{\Psi(:,2)}$ (i.e., every element in second column of matrix) and the elements of $\mathbf{D}_{\Psi(:,9)}$. The values in $\mathbf{D}_{\Psi(:,2)}$ change from approximately -30 to 10, but the range in $\mathbf{D}_{\Psi(:,9)}$ changes from -14×10^{13} to 2×10^{13}. The values of the matrix elements change from nearly zero to numbers of the order 10^{13} that are very large. Therefore, it leads to two problems; A matrix with large values results to highly computational cost, and with such distributed values creates bad condition.

If bad conditions are imposed on a matrix when it is reversed, some errors occur. Calculating an inverse matrix involves the division process, in machines (e.g., computers), accuracy of the division process effectively depend on types and values of accurate data. In a part of implementation of the primary algorithm, computing of $c = (\mathbf{D}_{\Psi}^{*T}\mathbf{D}_{\Psi}^{*})^{-1}(\mathbf{D}_{\Psi}^{*T}\ \Gamma_{F}^{*})$ necessitates the use of an inverse matrix. Because of the unfavorable values in matrix elements of $(\mathbf{D}_{\Psi}^{*T}\ \mathbf{D}_{\Psi}^{*})^{-1}$, this matrix is characterized by poor conditions and often produces errors in machine running. In turn, the phase matching algorithm performs ineffectively. When a matrix is close to singular, the calculation of an inverse matrix may contain ''garbage'' data. Such matrix is said to be in *bad condition* [23].

Therefore, the origin of problem is identified: the $\mathbf{D}_{\Psi}$ matrix. Now, we must modify the condition of $\mathbf{D}_{\Psi}$ matrix. Revising the modeling equation of group delay for filter H (i.e., λ_T) can eliminate the need to work with a wide range of

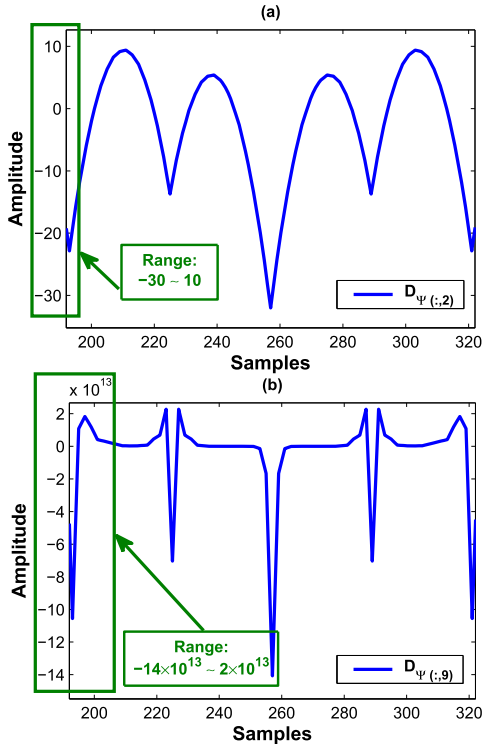

FIGURE 1. Two columns of D_Ψ matrix, for instance: (a) shows elements of 2nd and (b) shows elements of 9th column of D_Ψ obtained from primary algorithm.

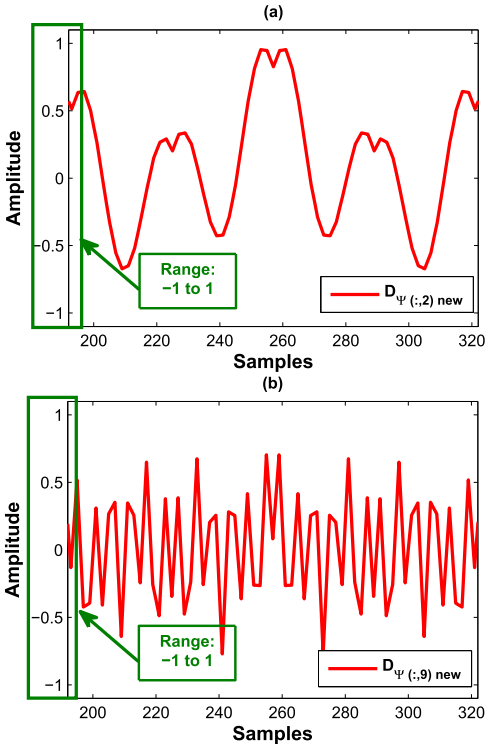

FIGURE 2. Two columns of D_Ψ matrix, for instance: (a) shows elements of 2nd and (b) shows elements of 9th column of D_Ψ obtained after proposed solution.

numbers, and matrices are created under the most favorable conditions. The λ_T model in the primary algorithm is an even and periodic function with an R-order polynomial function. We suggest the sine and cosine functions instead of the R-order polynomial function like to the sine and cosine in a Fourier series that can represent a function. Therefore, instead of using the (19), we propose the following relationship:

$$\lambda_T(\omega) = \sum_{r=0}^{R} c_r \cos(r\omega)\, \Pi\left(\frac{\omega}{2\pi}\right) \tag{30}$$

Because λ_T is even, however, the cosine term alone is sufficient. After discretizing and rewriting this relationship, elements of matrix $\mathbf{B}$ are obtained by

$$b_{n,r} = \sum_{k=-P/2}^{P/2-1} \cos(r(n-kT))\, \Pi\left(\frac{(n-kT)}{T}\right) \tag{31}$$

Because the proposed equation only affects the λ_T modeling, and it do not change the structure of the primary algorithm, so the prerequisites and properties of primary algorithm will not be changed. With this revision, matrices $\mathbf{B}$, $\mathbf{D}_\Psi$ and $\mathbf{D}_\Phi$ now have small values and much narrower ranges than those achieved using the primary algorithm.

To compare the modified algorithm and the primary algorithm, we return to the example in Fig. 1. As indicated in Fig. 2 by the results, the values in both $\mathbf{D}_{\Psi(:,2)}$ and $\mathbf{D}_{\Psi(:,9)}$ change from approximately -1 to 1, with only three or four floating digits. This indicates that the range of values is very minimal compared with that derived by the primary algorithm.

With this valuable modification in the primary algorithm, the phase matching process can do correctly and do not encounter with bad condition in the computation of inverse matrix. The error arising from poor matrix conditions is eliminated. The improvement of the matrix conditions is evaluated later in this paper. An interesting advantage of this revision is that, unlike the primary algorithm, which usually requires a value higher than 16 for the R order, the modified algorithm necessitates a considerably smaller R; usually, a value less than 8 suffices.

It is worth noting that this solution may not necessarily be a new technique, but the main contribution has been to discover and reveal problems which the primary algorithm suffers from them, and then to present an efficient solution.

B. WIDE LENGTH OF FILTERS AND SOLUTION

The generated length of wavelet filters in primary algorithm is very wide such as in [15], [16], and [19]; thus, applying DWT includes the highly computational costs. In many applications that generated wavelet coefficients is important, such as data compression by wavelet, or in applications with hardware constraints such as in bio-implant, the length of QMF has vital role. Having a wide length of filter for wavelet transform for many signals, such as neural signals recorded with numerous channels, image signals, etc. increases computational cost and is not desirable. As a reported solution in [15], after

obtaining the coefficients of h and g, the ineffective and small coefficients are removed, but the efficiency of wavelet transform is reduced; so this cut-off technique is not suitable trick. Therefore, the control over the length of QMF is necessary to have minimum numbers of generated wavelet coefficients. In the primary algorithm, there are not any controls over length of QMF. For example in [19] i.e. the origin of the primary algorithm, after design of matched wavelet for Daubechies-4 wavelet (*db4*) as a given signal, it has generated a wavelet with more than 32 coefficients, while *db4* has a known filter with 8-point of length.

The proposed method is as follows. At first, we use the algorithm to obtain $\Phi(\omega)$ and $\Psi(\omega)$, which have N-point of sampling frequency. In next step, to obtain appropriate length of filters for the wavelet function, we use a method that can be more clarified with a figure of an example. The example is dedicated to design of the wavelet for Daubechies-4 (*db4*) as a given signal. Using the primary algorithm, the amplitude of filters (i.e., $|H|$ and $|G|$) are obtained for a signal with a length of 512 points in Fast Fourier Transform (FFT), as Fig. 3(a). In function $|H|$, which exhibits low-pass behavior, therefore, $|H(e^{j\omega})|$ from a specified frequency (cut-off) is near to zero and has not any useful information. In this example, amplitude of $|H|$ is equal to zero in nearly 4th point.

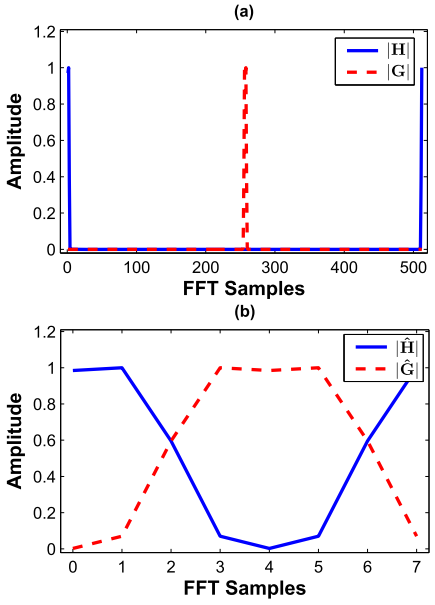

FIGURE 3. Creating QMF: a) $|H|$ and $|G|$ using primary algorithm, b) $|\hat{H}|$ and $|\hat{H}|$ using the proposed method.

With regard to $|H|$, it is obvious that in a wide range of frequencies, $|H|$ is zero. To delete the frequencies without any information we propose the picking out only the points with information. That is, instead of $|H(e^{j\omega})|$ in Fig. 3(a), the $|\hat{H}(e^{j\omega})|$ in Fig. 3(a) can be used. Now, instead of having a N-point FFT of h_k, we select TAP-point of it that are before cut-off frequency. This is equivalent to down-sampling concept. Therefore, new filter $\hat{H}_k$ is obtained from sampling of h_k, by a sampling rate that first frequency with zero amplitude occurs in TAP/2. Thus, sampling rate is N/TAP.

In briefly, the procedure is as following: To obtain TAP, firstly the FFT of h is computed. The first point where $|H(e^{j\omega})|$ is nearly equal to zero is equivalent to $\omega = \pi$ in discrete Fourier transform or the equivalent of TAP/2 in FFT with TAP-point. Then, the coefficients of filter h are sampled with a rate that provides the TAP-sample (i.e. N/TAP) and generates $\hat{H}_k$. The coefficients of $\hat{H}_k$ are normalized so that their sum is equal to $\sqrt{2}$. The new low-pass filter $\hat{H}_k$ is the final filter with minimum length of wavelet filter. Note that no information will be missing by using the proposed method with this down-sampling rate, because there are not any coefficients with important amplitude in deleted points (according to Fig. 3(a), from point 5 to 256).

Effects of the proposed approach on satisfaction of MRA conditions are discussed in Section V in details.

IV. RESULTS

A. A WELL-KNOWN WAVELET AS GIVEN SIGNAL

We selected *db4* as a given signal because it can visibly reflect the performance of the proposed approach by three reasons; firstly, it is a wavelet function itself, secondly it has the least possible filter length, thirdly it can serve as a signal for comparing results of this paper and results of the origin of the primary algorithm, i.e. [19]. The designed wavelet function and the coefficients obtained for $\hat{H}$ are shown in Fig. 4.

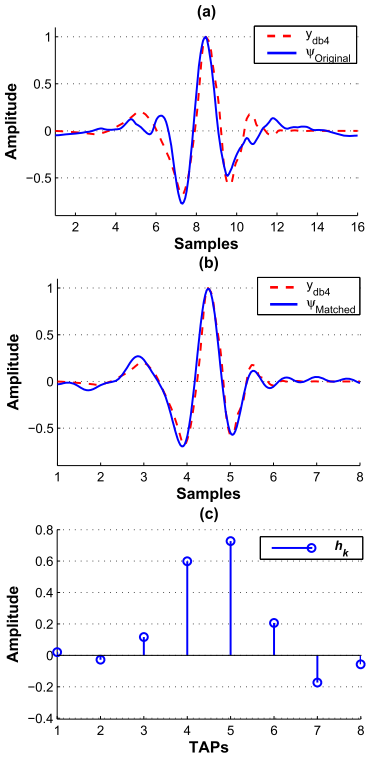

FIGURE 4. a) The given signal (y_{db4}) and matched wavelet using primary algorithm, b) Designed wavelet using proposed approaches, c) $\hat{H}$ filter for QMF using proposed approaches.

Compared with [19], the current study requires a considerably lower computational cost than that needed in [19] due to modified $\mathbf{D}_\Psi$ matrix. The current study also derives only 8 coefficients, which is identical to the number of coefficients derived for standard *db4* with the least of filter length. In [19], the number of coefficients is 32, and the authors removed the coefficients of sides, preserving only 16 central coefficients. Note, however, this procedure does not always work correctly. For example, in [15], wherein the authors removed filter coefficients with a wide range of 64 and preserved 20 central coefficients, however, removing the coefficients reported in the article creates significant errors. Thus, the proposed solutions examined with an actual wavelet as given signal, and it achieves to appropriate results for constructing matched wavelet with the least of filter length.

B. EXAMINATION OF SOLUTIONS WITH THE PUBLISHED STUDIES

Some studies e.g. in [15]–[17], have used the primary algorithm, but they obtained symmetric h and g, in the other words they have not-matched phase. In this examination, the proposed approach is evaluated for correctly phase matching process with performing on a signal of those studies. The selected signal used for examination is a ball-bearing failure signal [15], for which researchers set the phase of scaling function to zero. In these studies, h and g were symmetric and non-matched. As indicated in [15], the inner race fault in a deep groove ball-bearing generates a transient vibration signal that can be modeled by $y(t) = At^n\, exp(\text{-}Ct)sin(\omega_0 t)$, where $A = 68.74$, $n = 1.851$, $C = 6.78$, and $\omega_0 = 18.5$. The matching results of [15] suffer from two drawbacks: imperfect matching due to phase mismatch and wide length of filter, which was reported. For phase matching, the authors set the phase of scale function $\Phi(\omega)$ to zero and consequently derived h and g with real and symmetric coefficients, and the filter length was obtained 64. The wavelet function and filter coefficients obtained with the proposed approach are shown in Fig. 5. The proposed approach does not have those problems of [15], thus producing a wavelet that more accurately matches the given signal. In order to the simplification of calculations, the researchers in [15] used only 25 coefficients through filters. The proposed approach generates fewer filter coefficients (i.e., 20 versus more than 64). Improving the algorithm in [15] with respect to the aforementioned issues would have enhanced the performance of their approach.

C. AN APPLIED EXPERIMENT

In this section, the proposed approach is examined with an example from the real world. Implantable microsystems developed for electrically interfacing to the brain, nowadays, are of increasing interest to researchers in medical sciences, neuroscience, and engineering. When a microsystem records multiple channels, the designer encounters several challenges at some issues such as size and weight of the system, data bandwidth [24]. Techniques such as signal compression are the successful attempts reported to efficiently utilize the

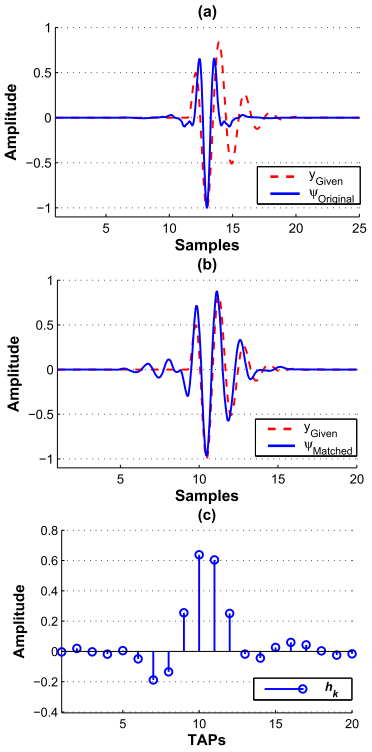

FIGURE 5. a) The given signal (ball-boring fault), and matched wavelet using primary algorithm, b) Designed wavelet using proposed approaches, c) $\hat{H}$ filter for QMF using proposed approaches.

limited available wireless transmission bandwidth. In many neural signal recording microsystem, the wavelet transform is used. Performance of a DWT-based compression approach is determined by the basis function used. Wavelet basis functions with more similarity to the general wave shape of neural spikes can approximate spikes with fewer coefficients. Therefore, designing of a matched wavelet is expectable to improve the overall system, that using spectral matching can be a candidate as method of designing. Nevertheless, using the primary algorithm cannot create the desired result, because of the mentioned drawback, i.e. the wide length of filters.

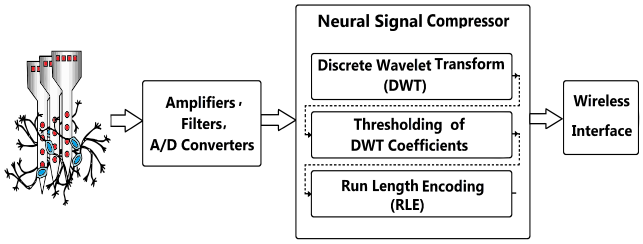

FIGURE 6. Simple block diagram of neural recording microsystem.

Fig. 6 shows the simplified block diagram of an implantable neural recording system. In the Implantable unit, the neural signal is recorded by microelectrodes, and then a circuitry block performs amplification, filtering, and digitizing [25].

In the Neural Signal Compressor block, the first step is transforming the signals by DWT. In the DWT domain, a few numbers of coefficients convey most of the energy of a neural signal, and the majority of the DWT coefficients are released without significant information. Then, by comparing the coefficients with a predefined threshold, coefficients under the threshold level are replaced by zeros, whereas other coefficients remained because they represent the most significant information in a neural signal. Finally, in the RLE block, non-zero values corresponding to above threshold level coefficients are moved to the output without any change, whereas zeroed coefficients are counted, and their number is moved. Therefore, the volume of data, which will be transmitted through the wireless link, is reduced. At the external unit of the implantable neural recording system, run length decoding and inverse of DWT reconstruct the neural signal.

This paper is only intended to examine the efficiency of proposed approach for designing of matched wavelet, so it is performed the compression process for single recording channel, and results can be extended to multi-channel. The current research uses the neural signals recorded by a microelectrode attached to the auditory cortex of a guinea pig's brain [26]. The spikes were extracted from the raw neural signals, after which a template signal was obtained by computing the average of the spikes. For the matched wavelet to the spike obtained through the proposed approach, the wavelet function and coefficients of $\hat{H}$ are shown in Fig. 7. This figure indicates that the number of filter coefficients is 8.

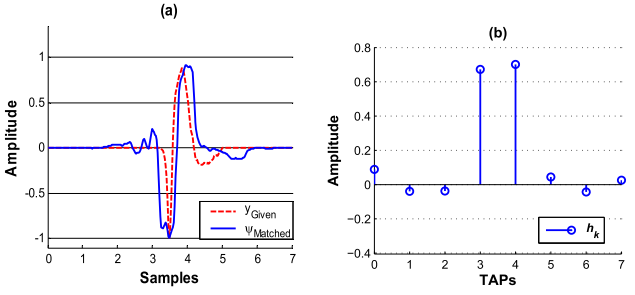

FIGURE 7. a) The designed matched wavelet $\psi(x)$, and given signal (neural spike), b: The $\hat{H}$ filter for QMF.

Two properties of the designed wavelet, i.e. to be matched and to have the least of filter length, present useful results in compression process. The efficiency of first property is illustrated in Fig. 8, where it shows partitions of the original and reconstructed signal. The background noise was removed sufficiently, and the spike was preserved with a negligible difference to original signal.

In general, the performance of compression process is evaluated by two criteria: error between original signal and reconstructed signal, and compression rate. The performance of the designed wavelet is shown by comparison with the other well-reported wavelet functions in literature such as

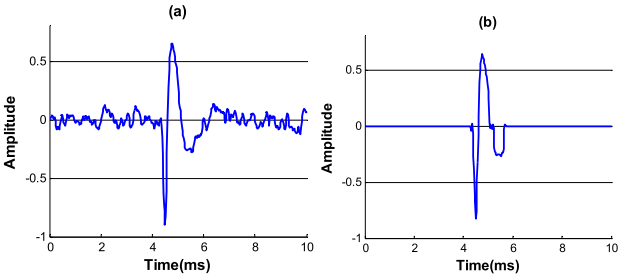

FIGURE 8. a) A part of the original spike with SNR=10dB, b) The reconstructed signal after compression process.

sym4, *db4, sym7* [22], [25], [26]. The normalized Root Mean Square (RMS) of the error was computed to indicate the difference between the spikes before and after compression. The RMS errors for *sym4*, *db4, sym7* and matched wavelet are 0.98%, 0.97%, 0.95%, 1.02%, respectively. These values indicate the errors are nearly 1% and difference between the errors is negligible. For the time being, the performance of the designed wavelet has been similar to general wavelets. However, the advantage of designed wavelet appears in the next criterion.

The compression rate of matched wavelet with well-reported wavelet functions is compared to show advantage of the designed wavelet with the least of filter length versus others. To measure the compression ability of the method, the compression ratio (CR) criterion defined as:

$$CR = \frac{N_B}{N_A}, \tag{32}$$

where N_B and N_A are the volumes of data before and after performing data compression, respectively. The comparison of CR in various signal-to-noise ratio (SNR) of input signal for *sym4*, *db4, sym7* and matched wavelet is shown in Fig. 9. The CR of the designed wavelet is more than the CR of the other well-reported wavelets. In high SNR, i.e. above 15dB, CR of the matched wavelet is 37 whereas CR of *sym4*, *db4, sym7* are 32, 26, 17, respectively.

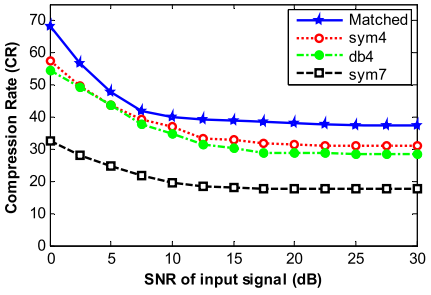

FIGURE 9. Compression Rate (CR) of the neural signals by using four wavelets: *sym4*, *sym7*, *db4* and matched wavelet.

In low SNR (nearly 0dB), difference of CR of the matched wavelet with others is more than 10, that it also indicates the designed wavelet is able to perform better than general wavelets in compression process with noisy situations.

In fact, the last result shows the matched wavelet can be used for other applications such as neural signal de-noising process, spike detection in noisy condition, etc. In those applications, the functionality of matched wavelet is expected to be better than general wavelets.

Therefore, this experiment indicated an applied example for the proposed approach in constructing of a matched wavelet based on an actual signal (neural spike). The designed wavelet is orthonormal and has the least possible length of filter and leads to highly proper results by comparison with the well-reported wavelets.

V. DISCUSSION

A. PERFORMANCE OF THE SOLUTION OF MATRIX CONDITIONS

With respect to the first problem (i.e., large range of numbers in the $\mathbf{D}_\Psi$ matrix and poor condition of it), the reduction of the range of numbers is illustrated in Fig. 2. With the proposed method, the reduction of amounts in matrices considerably decreases computational cost. The improvement in matrices can be validated by using some indicators. To verify the calculated inverse matrix, we use the *condition number* as an indicator. The condition number measures the sensitivity of a solution for a system of linear equations to input data error based on the singular value decomposition method. It computes the relationship between the smallest and largest eigenvalues, and its value falls between epsilon and 1. A condition number close to 1 indicates the good condition of matrix data. As the condition number in a matrix is close to epsilon, the conditions worsen and more errors occur in inverse matrix calculation.

The implementation of the primary algorithm to various examples indicates that the condition number is under 10^{-17}, even less, and it is far from one. Thus, the implementation of the algorithm naturally generates the following errors: ''matrix has bad conditions and the inverse matrix gives an error'' [23]. The proposed method achieves improvement in the condition number. For example, in the matched wavelet designed for *db4*, the condition numbers obtained for matrix $(\mathbf{D}_\Psi^{*T}\ \mathbf{D}_\Psi^{*})$ that is inverted in (27), are 6.036×10^{-18} by using the primary algorithm and 6.245×10^{-7} by using the proposed approach. These results show that using the proposed method realizes a considerable improvement in the order of 10^{10} and eliminates the error (also, the warning) arising from bad conditions.

B. CONCERN OF THE SOLUTIONS ON OMRA PROPERTIES

The most important property of the foundation that underlies the primary algorithm is the use of OMRA. As the number of coefficients of h and g filter decrease with the proposed approach, ensuring correctness requires the satisfaction of OMRA conditions. To strengthen the confidence that the coefficients reflect the appropriateness of the proposed approach, OMRA conditions are evaluated.

This section indeed tries to show the proposed approach can satisfy the OMRA conditions similar to the primary algorithm. In order to have an orthonormal wavelet filter with length of N-Tap, three following conditions must satisfy [27]. First equation satisfies normality of wavelet as following:

$$\sum_{k=1}^{N} \hat{h}_k = \sqrt{2} \tag{33}$$

The second condition satisfies orthogonality as:

$$\sum_{k=1}^{N} \hat{h}_k\, \hat{h}_{k-2n} = \delta_n, \quad n = 1, 2, ..., N \tag{34}$$

In case of $n = 0$, then $\sum \hat{H}_k = \sqrt{2}$ which this case is recalled as Square Normality condition. In other cases of n, they are recalled as Double Shift Orthogonality.

If vanishing moment is at least one, i.e. there is one zero at π in frequency response for wavelet then the third condition satisfies as follows:

$$\sum_{k=1}^{N} (-1)^k\ \hat{h}_{k+1} = 0 \tag{35}$$

Therefore, to survey the OMRA conditions four indicators can be computed. Normality for evaluation of normality condition, Square Normality and Double Shift Orthogonality for evaluation of orthogonality condition, and evaluation of vanishing moment as an extra condition. Table 1 presents the computed indicators for the presented examples in the previous section using the primary algorithm and the proposed approach.

TABLE 1. The obtained values of properties of orthonormal wavelet in OMRA for designed wavelets.

Specification	Given signal			
	db4		ball-bearing failure	
Reference	[19]	This Paper	[15]	This Paper
Length of filter	32	8	64	20
Normality	1.414	1.414	1.410	1.414
Square Normality	0.966	0.978	1.027	0.967
Orthogonality (Double Shift)	0.017	0.011	-0.016	0.016
Vanishing moment	-0.032	-0.029	0.010	-0.012

In spite of remarkable reduction in length of wavelet filters by the proposed approach, the Table 1 shows that indicators of the proposed approach have not considerable deviation from indicators of the primary algorithm. In other words, the proposed approach for constructing a wavelet with the least of filter length can satisfy the OMRA conditions similar to the primary algorithm. Therefore, not only the proposed approach does not degrade the OMRA condition, but also can considerably reduce the length of wavelet filter. On the contrary, [15] and [19] obtained large numbers of coefficients (64 and 32, respectively) and removed some coefficients, and obtained a final count

of 25 and 16 coefficients, respectively. Applying their cut-off method (i.e. eliminating side coefficients and preserving central coefficients) to reach minimum length of filter equal to coefficient numbers in this paper (i.e., 20 and 8, respectively) will degrade their OMRA conditions.

It may be seemed that the primary algorithm and consequently the proposed approach provide an approximate for generating the wavelet filters; However, with respect to Table 1, the error between values generated by the algorithms and ideal values is negligible. In fact, some part of this slight error is because of computational error not because of the algorithms, and other part of error can be because of low frequency sampling rate in mentioned examples.

VI. CONCLUSION

In different applications, using matched wavelets produces more favorable results than using general wavelets. An efficient algorithm for matched wavelets ensures that the band-limited frequency spectrum of a wavelet is directly matched to a specified signal, but it suffers from some problems. In this paper, these problems were introduced, and corresponding solutions were provided. Correctly spectral matching necessitates the matching of both phase and amplitude to a specified signal. The review of the literature shows that most of the studies that applied the algorithm for DWT failed to achieve full matching in the spectrum phase. The first problem is the heavy computation involved in spectral phase matching. This problem produces errors in machine running and consequently prevents the effective functioning of the phase matching algorithm. It is because calculating a matched phase requires working with matrices that have large numbers and bad conditions. By modification in primary algorithm, computational costs are significantly reduced, and by improving the condition number, we eliminated errors that were due to bad conditions of matrix. Such enhancements enabled correct phase matching. The second problem is the wide and uncontrollable nature of the length of filter generated for designed wavelets. This problem is crucial in applications with hardware constraints such as in implantable microsystems. For this problem, a proposed solution enabled us to generate orthogonal wavelet transform filters with the least of filter length. Using a practical experiment (neural spike compression), we showed the efficiency of the proposed solutions in deriving the least of filter length, improving the phase matching process, and ensuring effective spectral matching.

REFERENCES

[1] E. Pomponi, A. Vinogradov, and A. Danyuk, "Wavelet based approach to signal activity detection and phase picking: Application to acoustic emission," *Signal Process.*, vol. 115, pp. 110–119, Oct. 2015.

[2] M. Sharma, A. Dhere, R. B. Pachori, and V. M. Gadre, "Optimal duration-bandwidth localized antisymmetric biorthogonal wavelet filters," *Signal Process.*, vol. 134, pp. 87–99, May 2017.

[3] R. Gupta and R. Kapoor, "Data compression by discrete wavelet transform using matched wavelet," *Int. J. Signal Imag. Syst. Eng.*, vol. 8, no. 4, pp. 205–214, 2015.

[4] S. G. Mallat and Z. Zhang, "Matching pursuits with time-frequency dictionaries," *IEEE Trans. Signal Process.*, vol. 41, no. 12, pp. 3397–3415, Dec. 1993.

[5] R. R. Coifman and M. L. WickerHauser, "Entropy-based algorithms for best basis selection," *IEEE Trans. Inf. Theory*, vol. 38, no. 2, pp. 713–718, Mar. 1992.

[6] L.-K. Shark and C. Yu, "Design of matched wavelets based on generalized Mexican-hat function," *Signal Process.*, vol. 86, pp. 1451–1469, Jul. 2006.

[7] A. H. Tewfik, D. Sinha, and P. Jorgensen, "On the optimal choice of a wavelet for signal representation," *IEEE Trans. Inf. Theory*, vol. 38, no. 2, pp. 747–765, Mar. 1992.

[8] R. A. Gopinath, J. E. Odegard, and C. S. Burrus, "Optimal wavelet representation of signals and the wavelet sampling theorem," *IEEE Trans. Circuits Syst. II, Analog Digit. Signal Process.*, vol. 41, no. 4, pp. 262–277, Apr. 1994.

[9] R. Peeters and J. Karel, "Data driven design of an orthogonal wavelet with vanishing moments," in *Proc. 21st Int. Symp. Math. Theory Netw. Syst.*, Groningen, The Netherlands, 2014, pp. 1665–1672.

[10] R. C. Guido, J. F. W. Slaets, R. Köberle, L. O. B. Almeida, and J. C. Pereira, "A new technique to construct a wavelet transform matching a specified signal with applications to digital, real time, spike, and overlap pattern recognition," *Digit. Signal Process.*, vol. 16, pp. 24–44, Jan. 2006.

[11] A. Katunin and P. Przystałka, "Damage assessment in composite plates using fractional wavelet transform of modal shapes with optimized selection of spatial wavelets," *Eng. Appl. Artif. Intell.*, vol. 30, pp. 73–85, Apr. 2014.

[12] M. F. Mansour, "On the design of matched orthonormal wavelets with compact support," in *Proc. IEEE Int. Conf. Acoust., Speech, Signal Process. (ICASSP)*, May 2011, pp. 4388–4391.

[13] J. O. Chapa and R. M. Rao, "Algorithms for designing wavelets to match a specified signal," *IEEE Trans. Signal Process.*, vol. 48, no. 12, pp. 3395–3406, Dec. 2000.

[14] G. F. Takla, B. G. Nair, and K. A. Loparo, "Matching a wavelet to ECG signal," in *Proc. 28th Int Conf. IEEE EMBS Annu.*, New York, NY, USA, Aug./Sep. 2006, pp. 1686–1689.

[15] L. Tóth and T. Tóth, "On finding better wavelet basis for bearing fault detection," *Acta Polytechnica Hungarica*, vol. 10, no. 3, pp. 17–35, 2013.

[16] C. C. Fung and P. Shi, "Design of compactly supported wavelet to match singularities in medical images," *Proc. SPIE*, vol. 4790, pp. 358–370, Nov. 2002.

[17] M. D. Abolhassani, Y. Salimpour, A. Ahmadian, and V. Tavakoli, "Design of an optimized mother wavelet function for TEOAE signal denoising," in *Proc. 2nd IEEE Int. Conf. Bioinf. Biomed. Eng.*, May 2008, pp. 2032–2035.

[18] A. Gupta, S. D. Joshi, and S. Prasad, "A new method of estimating wavelet with desired features from a given signal," *Signal Process.*, vol. 85, pp. 147–161, Jan. 2005.

[19] J. O. Chapa, "Matched wavelet construction and its application to target detection," Ph.D. dissertation, Rochester Inst. Technology, Center Imag. Sci., Rochester, NY, USA, 1995.

[20] S. Mallat, *A Wavelet Tour of Signal Processing*, 2nd ed. New York, NY, USA: Academic, 1998.

[21] I. Daubechies, "Orthonormal bases of compactly supported wavelets," *Commun. Pure Appl. Math.*, vol. 41, no. 7, pp. 909–996, 1988.

[22] A. Salmanpour, L. J. Brown, and J. Shoemaker, "Spike detection in human muscle sympathetic nerve activity using a matched wavelet approach," *J. Neurosci. Methods*, vol. 193, pp. 343–355, Nov. 2010.

[23] MathWorks Inc. *MATLAB Software, Version 2015*. [Online]. Available: https://www.mathworks.com

[24] (2014). *United States Frequency Allocation Chart*. [Online]. Available: http://www.fcc.gov/encyclopedia /radio-spectrum-allocation

[25] K. G. Oweiss, A. Mason, Y. Suhail, A. M. Kamboh, and K. E. Thomson, "A scalable wavelet transform VLSI architecture for real-time signal processing in high-density intra-cortical implants," *IEEE Trans. Circuits Syst. I, Reg. Papers*, vol. 54, no. 6, pp. 1266–1278, Jun. 2007.

[26] S. Razmpour, A. M. Sodagar, M. Faizollah, M. Y. Darmani, and M. Nourian, "Reconfigurable biological signal co-processor for feature extraction dedicated to implantable biomedical microsystems," in *Proc. IEEE Int. Symp. Circuits Syst. (ISCAS)*, May 2013, pp. 861–864.

[27] K. P. Soman, *Insight Into Wavelets: From Theory to Practice*. New Delhi, India: PHI Learning, 2010.

MAHMOUD MANSOURI JAM received the B.Sc. degree in electrical engineering from Rajaee University, Tehran, Iran, in 2004, and the M.Sc. degree in electrical engineering from Shahed University in 2009, where he is currently pursuing the Ph.D. degree. His current research interests include signal processing (voice, image, and neural), wavelet designing, bio-implantable devices and systems, and microelectronics designing.

HAMED SADJEDI received the B.Sc., M.Sc., and Ph.D. degrees in electrical engineering from the Amirkabir University of Technology, Tehran, Iran, in 1995, 1997, and 2007, respectively. He is currently an Assistant Professor with Shahed University, Tehran. His research interests include biomedical signal and system processing, pattern recognition, DSP algorithms, and designing of hardware architecture (particularly in applications for hearing aid). He has tens of published papers in journals and proceedings, and three books in his research scope.